Ferroelectric-Mode Motion in KD_2PO_4†

J. SKALYO, JR., B. C. FRAZER, AND G. SHIRANE
Brookhaven National Laboratory, Upton, New York 11973
(Received 18 August 1969)

The atomic motions of the ferroelectric soft mode in KD_2PO_4 have been determined by neutron triple-axis spectrometry. Kaminow and Damen have investigated the ferroelectric mode in KH_2PO_4 and find it is overdamped, and Buyers *et al.* find the mode in KD_2PO_4 to be extremely overdamped. We have carried out an extensive study of this mode throughout both the [010] and [001] zones of the reciprocal lattice, and an energy analysis has indicated an inelasticity of less than 0.2 meV. The mode is not directly observable, as it superposes the Bragg peak, but a careful study of the temperature dependence of the compatible overdamped Σ_2 optic branch permitted an accurate determination of the ferroelectric mode intensity at the Γ points of 60 Brillouin zones. A least-squares calculation of the inelastic structure factors fits the intensities well, and this permitted an evaluation of the relative atomic movements. The model fit consisted of a linear combination of the seven modes spanning the Γ_3 representation as determined by Shur. The movement consists of K, P, and D atomic motions as proposed by Cochran from the structural studies of Bacon and Pease. In addition, a large z motion for the deuterium atoms and a large distortional motion in the x-y plane of the oxygen tetrahedra are observed.

I. INTRODUCTION

THE lattice dynamics of a crystal, intimately connected with the nature of the forces between the atoms, has been directly related to the phenomenon of ferroelectricity by Anderson[1] and Cochran.[2] It was shown that long-range Coulomb forces, arising from the dynamical movements of charge in ionic crystals, can cancel the short-range interatomic forces and lead to a lattice instability at the transition temperature. One may appropriately picture a particular transverse optic mode as having an associated "spring constant" that decreases to zero as the transition temperature is approached. The frequencies of the $\Gamma(\mathbf{q}=0)$ modes[3] are related to the static dielectric constant by a Lyddane-Sachs-Teller[4] relation which has been generalized to solids with more than two atoms per primitive cell by Cochran,[5]

$$\frac{\epsilon_0}{\epsilon_\infty}=\prod_i \frac{\omega_{i\mathrm{LO}}{}^2}{\omega_{i\mathrm{TO}}{}^2}, \tag{1}$$

where $\omega_{i\mathrm{LO}}$ and $\omega_{i\mathrm{TO}}$ are the longitudinal and transverse optical-phonon frequencies, respectively, and ϵ_∞ is the high-frequency dielectric constant.

If only one of the modes is varying with temperature, the temperature dependence can be related to the Curie-Weiss-type dependence of ϵ_0 by

$$\omega_0{}^2 \propto (T-T_0). \tag{2}$$

This mode, referred to as the ferroelectric mode, is a specific case of a "soft" mode occurring at the Γ point. Additionally, if the transition is of second order, the theory of Landau[6] predicts that only the ferroelectric mode will condense. In such cases, a rather restrictive relation between the mode motion and the symmetry of the high- and the low-temperature phase is implied.[7]

Soft modes have heretofore been extensively studied in crystals of the perovskite structure, the simplest known to exhibit ferroelectric behavior. The studies indicate that polymorphic phase changes can be well explained in these substances on the basis of condensing soft-phonon modes occurring at various symmetry points of the Brillouin zone. The behavior in this class of substances is diverse in that the ratio of the anharmonic imaginary frequency component to the undamped mode frequency varies over a wide range.

Kaminow and Damen[8] have utilized Raman-scattering measurements to study the ferroelectric mode in KH_2PO_4, and explained their results in terms of a mode frequency that is complex, i.e., $\omega=[\omega_0{}^2-(\frac{1}{2}\Gamma)^2]^{1/2}+\frac{1}{2}i\Gamma$. The mode was found to be overdamped ($\Gamma^2>2\omega_0{}^2$) with Γ independent of temperature and ω_0 decreasing to zero as the transition temperature is approached. As such measurements are made only at $\mathbf{Q}\simeq 0$, a picture of the mode motion cannot be given explicitly. Buyers *et al.*[9] have made triple-axis neutron-diffraction measurements on the ferroelectric mode in KD_2PO_4. It was noted that in the deuterated isomorph the mode is extremely overdamped ($\Gamma^2\gg 2\omega_0{}^2$), with frequency dependence as given by Eq. (2).

The present work is concerned with a detailed determination of the ferroelectric mode in KD_2PO_4 utilizing neutron spectrometry. The results of this study are in broad agreement with a dynamical model suggested by

† Work performed under the auspices of the U. S. Atomic Energy Commission.

[1] P. W. Anderson, *Proceedings of the Conference on the Physics of Dielectrics* (Academy of Science, USSR, Moscow, 1958), p. 290.

[2] W. Cochran, Advan. Phys. **9**, 387 (1960); **10**, 401 (1961).

[3] Notation after G. F. Koster, in *Solid State Physics*, edited by F. Seitz and D. Turnbull (Academic Press Inc., New York, 1957), Vol. 5, p. 201.

[4] R. H. Lyddane, R. G. Sachs, and E. Teller, Phys. Rev. **59**, 673 (1941).

[5] W. Cochran, Z. Krist. **112**, 465 (1959).

[6] L. D. Landau and E. M. Lifshitz, *Statistical Physics* (Addison-Wesley Publishing Co., Inc., Reading, Mass., 1958), p. 430.

[7] See, G. Y. Lyubarskii, *The Application of Group Theory in Physics* (Pergamon Press, Inc., New York, 1960), p. 121.

[8] I. P. Kaminow and T. C. Damen, Phys. Rev. Letters **20**, 1105 (1968).

[9] W. J. L. Buyers, R. A. Cowley, G. L. Paul, and W. Cochran, in *Neutron Inelastic Scattering* (International Atomic Energy Agency, Vienna, 1968), Vol. 1, p. 267.

Cochran[2] for the hydrogenous prototype KH_2PO_4, although there are some differences which may be significant in explaining the phase transition—at least in the deuterated case.

II. PRELIMINARY DETAILS

A. Crystal Structure

The structure of KH_2PO_4 has been determined by x-ray[10] and neutron[11] diffraction in both the paraelectric and ferroelectric phases. The paraelectric phase possesses space group symmetry $I\bar{4}2d$, with four molecules in the body-centered tetragonal unit cell. The important structural feature is the network of hydrogen bonds which links each phosphate group to neighboring phosphate groups in a tetrahedral array. An (001) projection of the structure is given in Fig. 1. The low-temperature structure is orthorhombic, $Fdd2$, with the primitive cell containing the same number of atoms as in $I\bar{4}2d$. The unit cell axes of $Fdd2$ in the a-b plane are rotated about the c axis by 45° with respect to the axes of $I\bar{4}2d$ and are of unequal length.

The hydrogen positions are indicated in the figure at the center of the bond between the two PO_4 tetrahedra. Actually, the length of the bond is rather critical in determining the positioning of the hydrogens.[12] The bond length of 2.52 Å, observed in KH_2PO_4, is in an ambiguous range where either a single anharmonic potential well or a double well with a low barrier may exist along the bond. On the basis of their neutron-diffraction data, Bacon and Pease[11] were not able to distinguish whether the hydrogen nuclei were making large anharmonic vibrations about the bond center point, or whether they were disordered in two wells. In the low-temperature phase, however, the hydrogens were observed to be in ordered off-center positions.

Blinc and Hadzi[13] have interpreted infrared data as due to a double-well potential with the protons tunneling through a low intermediate barrier. Blinc[14] has also used the tunneling concept to explain the isotope effect whereby deuteration increases the transition point from 120 to 220°K. The isotope effect was not explained on the basis of the Slater[15] or Takagi[16] statistical order-disorder interpretations. A pseudospin Ising-type model was employed by de Gennes[17] to describe the tunneling process. This approach initially neglected the interaction of the proton motion with the mode motion of the rest of the lattice. Tokunaga and Matsubara[18] subsequently showed how the results of the Slater-Takagi[15,16] statistical model could be derived from the tunneling model.

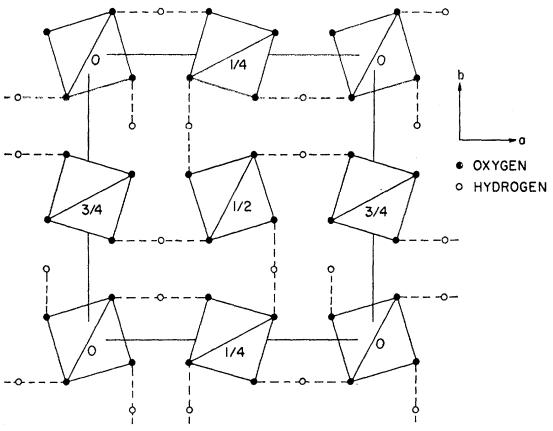

FIG. 1. An (001) projection of the structure of KH_2PO_4. The heights of the centers of the PO_4 tetrahedra are shown. The unit cell is outlined.

As the principal component of hydrogen motion is perpendicular to the polarization axis (c axis), it appears that neglect of the other atoms cannot give a quantitative description of the ferroelectric process. The x-ray data of Frazer and Pepinsky[10] and the neutron study of Bacon and Pease[11] both definitely establish that in the low-temperature phase the K and P atoms have opposite displacements parallel to the c axis relative to the oxygen tetrahedra; when all ionic displacements are considered, the polarization of the ferroelectric phase can be accounted for in a reasonable manner.

The inclusion of the proton-lattice interaction into the system Hamiltonian has been shown by Blinc and Ribaric[19] to substantially reduce the tunneling frequency, indicating the importance of such interactions in explaining the dynamics of the transition. Kobayashi[20] has extended the pseudospin tunneling model to permit coupling with the optical-mode movement of the K and P ions along the c axis. This yielded a coupled mode frequency which becomes soft in much the same manner as in the Cochran description.[2] It appears therefore that a definitive determination of atomic movements in the ferroelectric mode are necessary for an understanding of the transition.

Cochran[2] utilized the structure analysis of Bacon and Pease[11] in a model description of the ferroelectric-mode motion in KH_2PO_4. As the transition is very nearly second order, the difference between the high- and low-temperature structure was attributed to the condensed mode. This motion, depicted in Fig. 2, may be regarded in terms of stationary oxygen tetrahedra with hydrogen atoms moving in the a-b plane; the P and K atoms move along the c axis opposite to each other. This model was

[10] B. C. Frazer and R. Pepinsky, Acta Cryst. **6**, 273 (1953).
[11] G. E. Bacon and R. S. Pease, Proc. Roy. Soc. (London) **A230**, 359 (1955); **A220**, 397 (1953).
[12] W. C. Hamilton and J. A. Ibers, *Hydrogen Bonding in Solids* (W. A. Benjamin, Inc., New York, 1968), p. 52.
[13] R. Blinc and D. Hadzi, Mol. Phys. **1**, 391 (1958).
[14] R. Blinc, J. Phys. Chem. Solids **13**, 204 (1960).
[15] J. C. Slater, J. Chem. Phys. **9**, 16 (1941).
[16] Y. Takagi, J. Phys. Soc. Japan **3**, 271 (1948).
[17] P. G. de Gennes, Solid State Commun. **1**, 132 (1963).
[18] M. Tokunaga and T. Matsubara, Progr. Theoret. Phys. (Kyoto) **35**, 581 (1966).
[19] R. Blinc and M. Ribaric, Phys. Rev. **130**, 1816 (1963).
[20] K. Kobayashi, J. Phys. Soc. Japan **24**, 497 (1968).

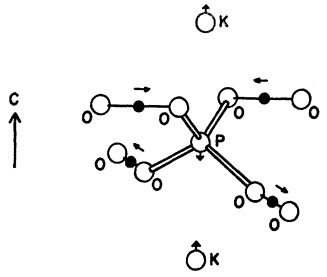

FIG. 2. Ferroelectric-mode motion as depicted by Cochran based on structural studies of the transition by Bacon and Pease.

used as a starting point in the analysis of neutron data in the present work.

B. Neutron Scattering

The neutron-scattering cross section for creation or annihilation of a phonon with a complex frequency can be written as

$$\frac{d^2\sigma}{d\Omega d\omega} \propto \frac{|\mathbf{k}_f|}{|\mathbf{k}_i|}|F_i(\mathbf{Q})|^2[n(\omega)+1]\frac{\omega\Gamma}{(\omega_0^2-\omega^2)^2+(\omega\Gamma)^2}, \quad (3)$$

where $\hbar\mathbf{Q}=\hbar(\mathbf{k}_f-\mathbf{k}_i)$ is the momentum transfer, $\hbar\omega$ is the energy transfer, and Γ is the imaginary part of the mode frequency. The phonon occupation number is

$$n(\omega)=(e^{\hbar\omega/kT}-1)^{-1}, \quad (4)$$

and $F_i(\mathbf{Q})$ is the inelastic-structure factor. In the limit $kT\gg\hbar\omega$, the cross section becomes

$$\frac{d^2\sigma}{d\Omega d\omega} \propto \frac{|\mathbf{k}_f|}{|\mathbf{k}_i|}|F_i(\mathbf{Q})|^2\frac{kT}{\hbar}\frac{\Gamma}{(\omega_0^2-\omega^2)^2+(\omega\Gamma)^2}. \quad (5)$$

The cross section has two peaks for $\Gamma^2<2\omega_0^2$ and only one peak at $\omega=0$ for $\Gamma^2\geq 2\omega_0^2$. The energy profiles for various values of $\Gamma/2\omega_0$ are shown in Fig. 3 for positive values of ω. The profile peaks at $\pm\omega_0$ for $\Gamma/2\omega_0\ll 1$ and peaks very sharply at $\omega=0$ for $\Gamma/2\omega_0\gg 1$. The integrated intensity in all cases is

$$\frac{d\sigma}{d\Omega} \propto |F_i(\mathbf{Q})|^2\frac{T}{\omega_0^2}, \quad (6)$$

with a quasi-elastic energy broadening of $2\hbar\omega_0^2/\Gamma$ occurring for $\Gamma/2\omega_0\gg 1$.

The inelastic-structure factor $F_i(\mathbf{Q})$ is given by

$$F_i(\mathbf{Q}) \propto \sum_j b_j(\mathbf{Q}\cdot\xi_j)e^{i\mathbf{Q}\cdot\mathbf{r}_j}\exp\left(-\frac{\mathbf{Q}\cdot\mathbf{B}_j\cdot\mathbf{Q}}{16\pi^2}\right), \quad (7)$$

where j is summed over the atoms of the unit cell. $\mathbf{B}_j$ is the anisotropic Debye-Waller factor, $\mathbf{r}_j$ is the position in the unit cell, and b_j is the scattering length of the jth atom. Equation (7) is the usual elastic-structure factor except for the term $(\mathbf{Q}\cdot\xi_j)$ where ξ_j is the mode displacement vector of the jth atom. The integrated scattering intensity of a phonon with wave vector $\mathbf{q}=\mathbf{Q}-\mathbf{G}$ ($\mathbf{G}$ is a reciprocal lattice vector) therefore varies throughout the extended zone. It is therefore possible to determine the ξ_j by making phonon intensity measurements for a particular $\mathbf{q}$ throughout reciprocal space and utilizing standard fitting procedures to Eq. (7).

Several reflections of the ferroelectric mode were measured by Buyers *et al.*,[9] too few to attempt a least-squares fit, and resulted in substantially poor agreement with mode vectors as depicted in Fig. 2. As the Cochran mode is fundamental to many theoretical approaches of ferroelectricity in KH_2PO_4 and its isomorphs, the work of Buyers *et al.*[9] is therefore extended here to measurements of the ferroelectric-mode intensities throughout the [010] and [001] zones of KD_2PO_4.

III. FERROELECTRIC-MODE SYMMETRY

The displacements that occur for a particular phonon mode can, in general, be described by n complex displacement vectors; i.e., one for each of the n atoms in the primitive cell. At the Γ point, however, the displacement vectors can be chosen as real because of time reversal symmetry, thus halving the number of unknown parameters. While the measurement of these eigenvectors can be made for particular modes of a multiatomic crystal, the measurement and description of complete phonon spectra is not physically feasible at present. The measurement of particular modes which bear an intimate relation with a polymorphic or ferro-

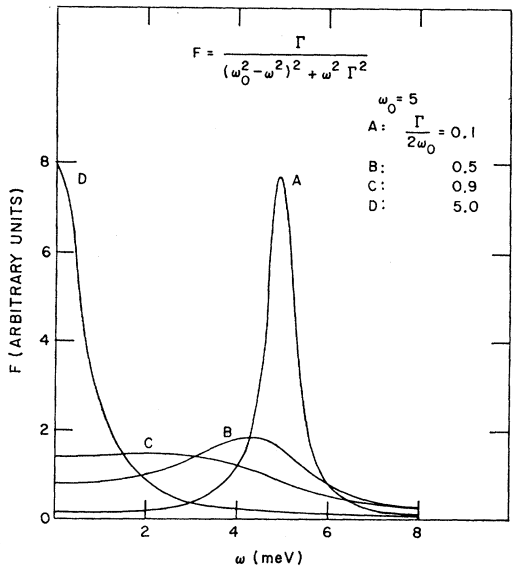

FIG. 3. Frequency distribution of a phonon as a function of different strength-damping parameters. The particular case of KD_2PO_4 is similar to curve D.

electric phase change does, however, present a tractable undertaking.

Such soft modes must occur at **q** values with point symmetry permitting more than just the identity operator; the soft modes can therefore not occur at general points of the Brillouin zone.[7] In particular, the ferroelectric mode occurs at the Γ point, which allows one to take full advantage of the point group symmetry of the crystal. Group-theoretical restrictions can therefore greatly simplify the form of the dynamical matrix and of its eigenvectors. Extensive reviews of the implications of group theory and its application to the symmetry properties of phonon modes, replete with examples, have been made by Maradudin and Vosko[21] and by Warren.[22] Utilizing recipes given therein, along with a tabulation by Kovalev[23] of the irreducible multiplier representations of the point groups, allows symmetry restricting information to be calculated for a phonon in any crystal structure.

For the particular case of KD_2PO_4, there are two molecules in the primitive cell resulting in 48 modes for each **q** value. Shur[24] has calculated the number of modes for each irreducible representation at symmetry points of the KH_2PO_4 structure above and below the transition temperature. Additionally, he has depicted a set of basis vectors for each of the representations of the Γ point. Any mode of a particular symmetry representation can then be found as a linear combination of the basis vectors spanning the irreducible representation. The number of modes in each representation of the high-temperature phase is[25] $\Gamma_1=4$ modes, $\Gamma_2=5$ modes, $\Gamma_3=7$ modes, $\Gamma_4=6$ modes, $\Gamma_5=13$ doubly degenerate modes.

The ferroelectric mode is in the Γ_3 representation, and three of the seven basis vectors are depicted in Fig. 4. The other four basis vectors of Γ_3 are of the type whereby all atoms of a like kind move along the c axis with equal amplitude and phase. An acoustic mode is thus of Γ_3 symmetry and is merely a combination of the latter four basis vectors. This fact has the additional benefit of reducing the number of unknown amplitudes by one, as the ferroelectric mode must be orthogonal to the acoustic mode. It is also clear that the Cochran mode, as illustrated in Fig. 2, is a particular linear combination of the seven modes. It is also evident that if the ferroelectric mode condenses, then only a Γ_3 mode can produce the symmetry of the low-temperature phase, viz., become a Γ_1 mode of the low-temperature phase.[26] As the overdamped ferroelectric mode at $\mathbf{q}=0$ superposes the Bragg peak, the branch containing this mode will be studied at finite **q**. In particular, the Γ_3 mode is compatible with Σ_2 and Λ_1 symmetry.

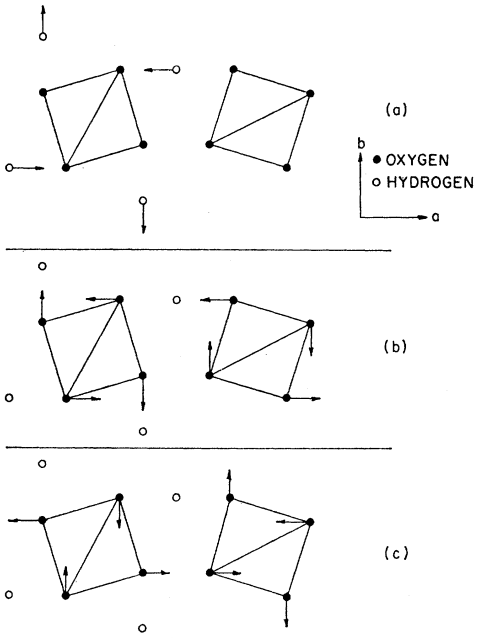

FIG. 4. Three of the seven basis vectors spanning the Γ_3 representation as determined by Shur. Only the atoms contained in one primitive cell are depicted, and their relation to the unit cell can be seen by comparison with Fig. 1.

KD_2PO_4 and KH_2PO_4 are piezoelectric and measurements of $C_{66}{}^E$ indicate anomalous behavior of the acoustic mode.[27–29] Cochran[22] has interpreted this as an interaction of the ferroelectric branch with an acoustic branch of similar symmetry at small **q**. Because of the noncrossing of branches of like symmetry, the decreasing energy of the ferroelectric branch pushes the acoustic mode down in energy near $\mathbf{q}=0$. An elastic instability occurs when the slope of the acoustic branch at $\mathbf{q}=0$ becomes zero thus initiating the phase change. The first-order nature of the transition is due here to the fact that the ferroelectric mode frequency is not yet zero at the transition. The mode which interacts with the ferroelectric branch is the Σ_2 mode transforming as y; viz., the transverse acoustic mode with polarization parallel to the y axis.

The Γ_3 acoustic mode is compatible with Σ_2 and Λ_1 modes. The other two translational modes are contained in the doubly degenerate Γ_5 representation. These modes are compatible with the degenerate modes Λ_3 and Λ_4 along [001] and with Σ_1 and Σ_2 along [100].

[21] A. A. Maradudin and S. H. Vosko, Rev. Mod. Phys. **40**, 1 (1968).
[22] J. L. Warren, Rev. Mod. Phys. **40**, 38 (1968).
[23] O. V. Kovalev, *Irreducible Representations of the Space Groups* (Gordon and Breach Science Publishers, Inc., New York, 1965).
[24] M. S. Shur, Kristallografiya **11**, 448 (1966); **12**, 215 (1967) [English transls.: Soviet Phys.—Cryst. **11**, 394 (1966); **12**, 181 (1967)].
[25] Subscripts refer to representations as given by Kovalev in Ref. 23.
[26] J. L. Birman, Phys. Rev. Letters **17**, 1216 (1966).
[27] W. P. Mason, Phys. Rev. **69**, 173 (1946).
[28] E. Litov and E. Uehling, Phys. Rev. Letters **21**, 809 (1968).
[29] E. M. Brody and H. Z. Cummins, Phys. Rev. Letters **21**, 1263 (1968).

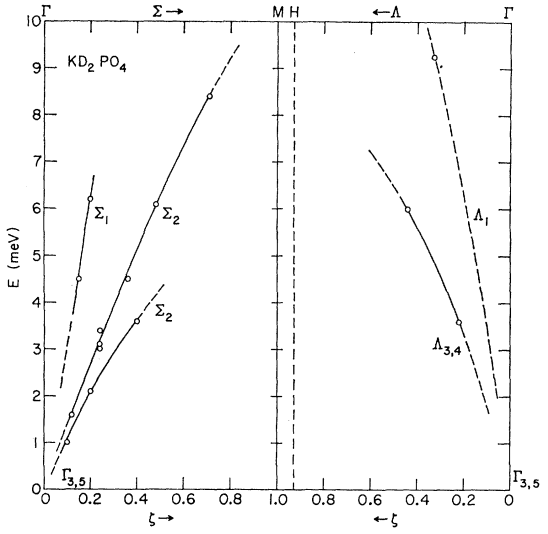

FIG. 5. Acoustic phonon branches of KD_2PO_4. Λ_3 and Λ_4 are degenerate. The Σ_1 branch and the lowest-lying Σ_2 branch were measured in an [001] zone while the others were measured in an [010] zone.

IV. EXPERIMENTAL

A. Sample and Spectrometer

Two KD_2PO_4 crystals were used in the present measurements. The [010] zone measurements were made on a crystal with dimensions 10, 20, and 10 mm along the a, b, and c axes, respectively. It has a specified deuteration of 99% and had a measured transition temperature of 221°K, in agreement with previously reported results.[30] The [001] zone measurements were made on a crystal 25 mm on each side, with cube edges parallel to the crystal axes. This crystal also had a specified deuteration of 99%, but the transition temperature was not measured as both crystals were from the same source.[31] The mosaic spread of both samples was less than 12 min. The crystals were mounted in sealed holders with helium gas to promote thermal equilibrium during measurements. The sample holders were mounted in a cryostat capable of temperature regulation to within ±0.1°K.

Neutron intensity measurements were made at the Brookhaven High Flux Beam Reactor on a triple-axis spectrometer. Germanium crystals were utilized as both monochromator and analyzer, and either the (111) or (311) reflections were used. The effective collimation was 20 min before and after the sample, and the initial energy of the neutron beam varied, depending on the nature of the particular measurement.[32] Good energy resolution, needed to determine the inelasticity of the ferroelectric mode, required a low initial energy of 13 meV. Most measurements were concerned with surveying the intensity of the Σ_2 ferroelectric branch in the [010] zone, and initial energies of 13, 20, 30, 50, and 70 meV were utilized as needed to permit observations at large **Q**.

B. Initial Survey

As the ferroelectric mode is overdamped[9] and superposes the Bragg peak, the amplitude of the Σ_2 ferroelectric branch must be studied as a function of **q**. An extrapolation to $\mathbf{q}=0$ can then be taken as the ferroelectric mode intensity. In order to obtain reliable intensity data, measurements must be carried out as closely as possible to the Bragg peak, while taking care that acoustic-phonon modes are not being detected due to the finite energy resolution of the spectrometer.[32] The acoustic-phonon branches were therefore measured at 250°K in the vicinity of the Γ point along the [100] and [001] directions. These results are shown in Fig. 5.

All of the branches are located well away from $E=0$ except in the immediate neighborhood of the Bragg peak. The two acoustic Σ_2 branches were also observed at a few temperatures between the transition and room temperature, and no measurable energy shift was detected. Particular attention was given the Σ_2 branch measured in the [001] zone, since this mode relates to C_{66} (the elastic constant which behaves anomalously when measured at constant applied field).

Measurements of C_{66} by neutron spectroscopy by Cowley *et al.*[33] indicate that the neutron measurements

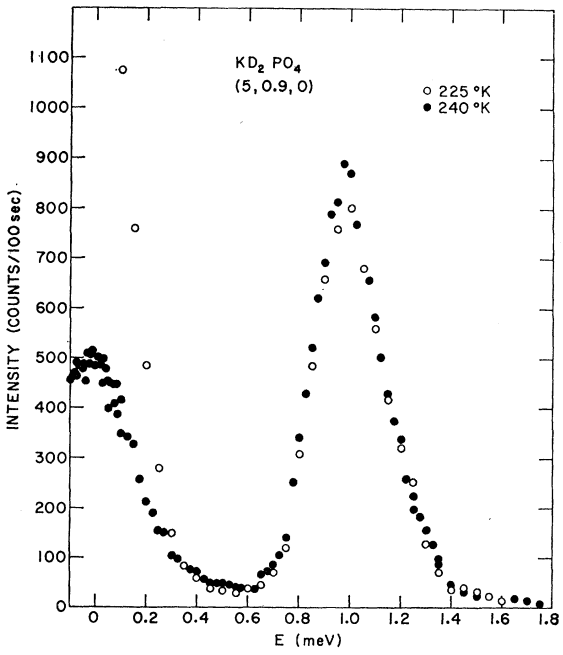

FIG. 6. Σ_2 acoustic phonon measured in the [001] zone. The peak near $E=0$ is due to the overdamped ferroelectric branch Σ_2 phonon.

[30] T. R. Sliker and S. R. Burlage, J. Appl. Phys. **34**, 1837 (1963).
[31] Clevite Corporation, Cleveland, Ohio.
[32] M. J. Cooper and R. Nathans, Acta Cryst. **23**, 357 (1967).
[33] R. A. Cowley, W. J. L. Buyers, E. C. Svensson, and G. L. Paul, in *Neutron Inelastic Scattering* (International Atomic Energy Agency, Vienna, 1968), Vol. 1, p. 281.

are more akin to C_{66}^D rather than the anomalous C_{66}^E. Highly accurate measurements with particularly precise energy resolution were made of the mode at (5,0.9,0) with the spectrometer closely focused to the slope of the dispersion curve.[32] These scans are depicted in Fig. 6 for measurements at 225 and 240°K. The measurements indicate an energy of 1.00±0.02 meV with a relative change in energy of less than 0.5% with temperature. This results in a value for C_{66} of (7.7±0.3) $\times 10^{10}$ dyn/cm^2, some 20% higher than obtained by Cowley *et al.*[33]

In principle, measurements of the quasi-elastic energy broadening of the Σ_2 ferroelectric branch, $2\hbar\omega_0^2/\Gamma$, as a function of temperature can give the temperature dependence of Γ when combined with the temperature dependence of ω_0^2 determined by Buyers *et al.*[9] An energy analysis of the overdamped Σ_2 branch was made at several $\mathbf{q}$ values and temperatures at high resolution near both (303) and (510). A portion of such a scan is shown near $E=0$ in Fig. 6. All such measurements resulted in line shapes, in agreement with instrumental resolution, as calibrated by incoherent scattering from vanadium. Thus the measurements set an upper limit of the inelasticity as being less than 0.2 meV. A beneficial result of this small inelasticity is that scans of the Σ_2 ferroelectric branch intensity as a function of $\mathbf{q}$ need be done only with the spectrometer set at $E=0$.

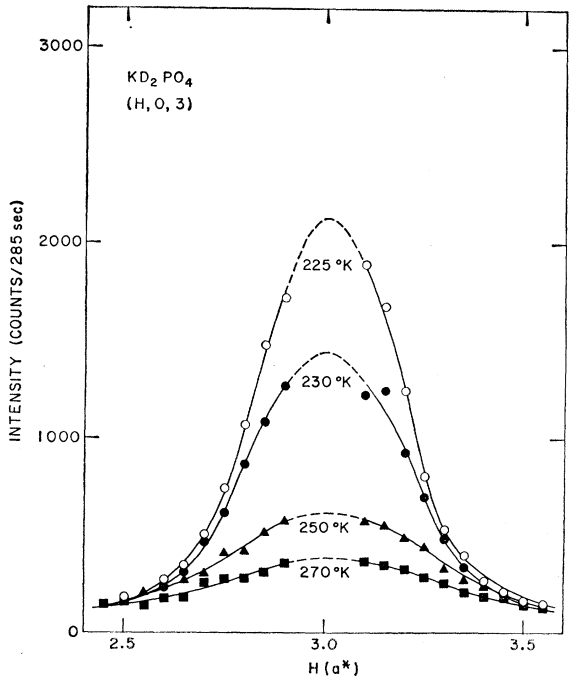

FIG. 7. Scan at $E=0$ of the temperature dependence of the overdamped ferroelectric branch Σ_2 phonon measured in the [010] zone near (303).

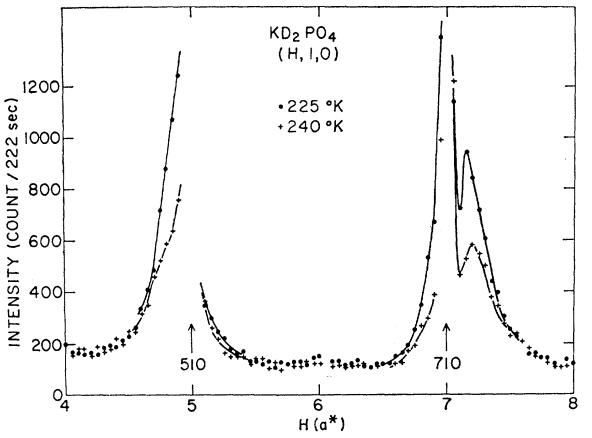

FIG. 8. Scan at $E=0$ of the temperature dependence of the overdamped ferroelectric branch Σ_2 phonon measured in the [001] zone near (510) and (710).

C. Σ_2 Ferroelectric Branch

The intensity of the Σ_2 ferroelectric branch was measured throughout the extended [010] and [001] zones. Measurements were made at 225 and 240°K and the difference was taken as the ferroelectric branch intensity. This precludes the possibility that the intensity might be due in part to another non-temperature-dependent overdamped phonon branch. The intensity near (303) is shown as a function of temperature in Fig. 7. The curves vary smoothly over the zone and an extrapolation to the zone center giving the ferroelectric-mode intensity is possible.

The shape of the curves near all of the Bragg peaks in the [010] zone was similar in appearance to those of Fig. 7, though of varying intensity. To allow as close an approach as possible to the Bragg peak, the initial neutron energy was kept as small as possible consistent with attaining physically permissible scattering angles on the spectrometer. The intensity of the most intense zone, (303), was measured at all energies and utilized for normalization purposes.

A typical measurement taken in the [001] zone is shown in Fig. 8. The intensity is observed to vary asymmetrically in the vicinity of the Γ points, thus precluding a suitable extrapolation to $\mathbf{q}=0$. This asymmetry prevailed throughout the [001] zone where the ferroelectric branch gave a finite intensity. Reliable zero intensity observations were, however, made at (110), (330), and (550). It was therefore possible to use only [010] zone measurements in the mode analysis, and a summary of the extrapolated intensities $I(\mathbf{q}=0)$ is given in Table I for the various Brillouin-zone Γ points.

The intensity of an overdamped phonon as given by Eq. (6) indicates the observations are dependent on the combined $\mathbf{Q}$ dependence of both ω_0 and $F_i(\mathbf{Q})$. The asymmetric intensities of Fig. 8 are due, however, only

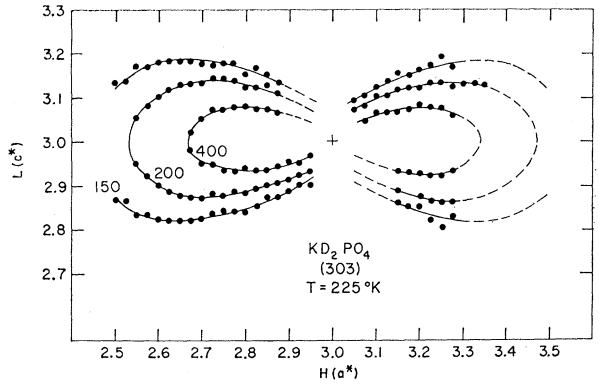

FIG. 9. Intensity contour in the [010] zone near (303) observed with $E=0$.

to a large variation in $F_i(\mathbf{Q})$, since $\omega_0(\mathbf{Q})=\omega_0(\mathbf{q})$ and is periodic with the symmetry of the lattice. Further evidence of the large variation in $F_i(\mathbf{Q})$ for the [001] zone measurements is depicted in Figs. 9 and 10 where intensity contours of the overdamped mode are shown for measurements made near (303) and (510), respectively. Additional contours taken near (301) and (220) confirmed that $F_i(\mathbf{Q})$ varies in a manner permitting reliable extrapolations only in the [010] zone. Representative calculations of the effect of finite resolution on the contours indicate significant disturbances only in the immediate vicinity of the Bragg peak, i.e., $|\mathbf{q}|<0.05$ Å^{-1}.

TABLE I. Ferroelectric mode observed intensities and intensities calculated by Eq. (8) utilizing the mode amplitudes of Table II (arbitrary units).

(h,k,l)	$I(\mathbf{q}=0)$	$\lvert F_c\rvert^2$	(h,k,l)	$I(\mathbf{q}=0)$	$\lvert F_c\rvert^2$
2, 0, 0	<1	0	1, 0, 5	5±5	3
4, 0, 0	<1	0	3, 0, 5	5±5	3
6, 0, 0	<1	0	5, 0, 5	47±10	44
8, 0, 0	<1	0	7, 0, 5	44±6	30
10, 0, 0	<2	0	9, 0, 5	68±8	62
12, 0, 0	<2	0	11, 0, 5	<6	2
1, 0, 1	<3	1	0, 0, 6	<2	0
3, 0, 1	20±2	24	2, 0, 6	4±2	2
5, 0, 1	41±2	43	8, 0, 6	4±6	3
7, 0, 1	65±4	63	10, 0, 6	15±12	2
9, 0, 1	28±3	29	1, 0, 7	49±10	42
11, 0, 1	13±9	16	3, 0, 7	17±4	18
0, 0, 2	<1	0	5, 0, 7	75±9	61
2, 0, 2	2±1	1	7, 0, 7	7±6	0
4, 0, 2	5±2	6	9, 0, 7	16±9	6
6, 0, 2	8±4	7	2, 0, 8	10±10	19
8, 0, 2	<2	1	4, 0, 8	<9	0
10, 0, 2	7±6	0	6, 0, 8	28±6	1
12, 0, 2	3±6	0	8, 0, 8	13±6	0
1, 0, 3	<2	4	1, 0, 9	9±9	20
3, 0, 3	84±3	80	3, 0, 9	<9	2
5, 0, 3	35±3	33	5, 0, 9	<9	2
7, 0, 3	32±3	36	7, 0, 9	62±9	57
9, 0, 3	9±4	5	2, 0, 10	10±6	1
11, 0, 3	15±6	17	4, 0, 10	9±6	15
2, 0, 4	5±5	18	6, 0, 10	21±6	29
4, 0, 4	15±3	0	1, 0, 11	<9	1
6, 0, 4	9±4	0	3, 0, 11	50±6	59
8, 0, 4	5±3	0	1, 1, 0	<1	0
10, 0, 4	4±6	5	3, 3, 0	<1	0
			5, 5, 0	<1	0

V. MODE ANALYSIS

A least-squares calculation was utilized to fit the observed [010] zone intensities of Table I to the equation

$$I(\mathbf{Q},\mathbf{q}=0)=k\left|\sum_j b_j(\mathbf{Q}\cdot\boldsymbol{\Delta}_j)e^{i\mathbf{Q}\cdot\mathbf{r}_j}\times\exp\left(-\frac{\mathbf{Q}\cdot\mathbf{B}_j\cdot\mathbf{Q}}{16\pi^2}\right)\right|^2, \quad (8)$$

where k is a scale factor fixed at a value that gave the deuterium atoms an amplitude similar to the x-y displacement the hydrogens experience at the transition in KH_2PO_4. All amplitudes are therefore relative. The $\boldsymbol{\Delta}_j$ are merely displacements of the jth atom obtained by a linear combination of the seven modes of the Γ_3 representation. Whereas the K and P motions involve one amplitude each, the oxygen motion involves three and the deuterium has two amplitudes. The parameters are therefore K_z, P_z, O_z, D_z, D_a, O_b, O_c, where the latter three parameter subscripts refer to the modes as depicted in Fig. 4. The orthogonality to the acoustic Γ_3 mode requires the c.m. to remain fixed thus relating the first four parameters by

$$m_kK_z+m_pP_z+4m_0O_z+2m_dD_z=0. \quad (9)$$

The modes depicted in Fig. 4 automatically leave the c.m. fixed.

The values of the scattering lengths[34] were $b_p=0.51$, $b_k=0.37$, $b_0=0.577$, and $b_d=0.621$ (in units of 10^{-12} cm). The values for $\mathbf{r}_j$ were taken to be the same as given by Bacon and Pease[11] for the paraelectric phase of KH_2PO_4 at 132°K. Here, however, we place the deuterium in the symmetry position along the O—D—O bond rather than in the disordered positions given therein. The Debye-Waller factor used in the analysis was isotropic for the K, P, and O atoms. The Bacon and Pease[11] room-temperature measurements were utilized with their measurements at 132°K to give estimates of the Debye-Waller factor at 225°K. The values of B used were 0.92, 0.73, and 0.95 Å^2, respectively, for K, P, and O.

In the case of deuterium, the anisotropic Debye-Waller factor is probably different than for hydrogen and it was therefore introduced as a parameter. The parameter for the deuterium atom can be written as

$$\mathbf{B}_d=\begin{bmatrix}B_{11} & 0 & B_{13}\\ 0 & B_{22} & 0\\ B_{13} & 0 & B_{33}\end{bmatrix}$$

[34] The Neutron Diffraction Commission, Acta Cryst. **A25**, 391 (1969).

for the atom at (0.25, 0.148, 0.125). Certain elements are zero because of the symmetry of the position. Following Bacon and Pease,[11] a simplified $\mathbf{B}_d$ was chosen with $B_{13}=0$ and with the eigenvalues perpendicular to the O—H—O bond being similar, i.e., $B_{22}=B_{33}$. The experimental data are therefore fitted to six amplitudes, B_{11} and B_{22}.

A preliminary search was conducted by systematic calculation of the weighted sum of the squares of the deviations for approximately 10^6 different models, with tabulation of results only when the sum was lower than any previously obtained value. Thus provided with a good initial-solution point, the least-squares routine required but a few interations to converge adequately. In retrospect, it is felt that this search may have been unnecessary and that the accuracy of the initial guess is not as restrictive in determining mode solutions as that ordinarily necessary in a crystal-structure analysis. The fit resulted in a weighted variance of 2.1 and a list of the results is given in Table II. The positive signs for D_a, O_b, O_c are for motions as depicted in Fig. 4. The correlation matrix indicated no correlations between parameters greater than 0.6 except for a value of 0.82 between B_{11} and D_a. The calculated values of $|F_i(\mathbf{Q})|^2$ are given in Table I for comparison with the observed intensities.

As the measured transition temperature indicates the sample is highly deuterated, we have neglected the effect on the scattering length resulting from slight hydrogen contamination. It is noted that the evaluated deuterium amplitudes are inversely proportional to the scattering length and would therefore be increased insignificantly. The amplitudes of the other atoms are negligibly affected by even large changes in b_d.

The mode analysis has been achieved by utilizing a harmonic form for $F_i(\mathbf{Q})$. The neglect of multiphonon-interference effects[35] appears justified by the good fit obtained. However, as a check on possible effects due to anharmonicity, the data were also analyzed in two groups depending on $\mathbf{Q}$ being less than or greater than 7 Å^{-1}. The results were substantially unaltered except for the parameters O_z and D_z as determined from the group with $\mathbf{Q}<7$ Å^{-1}. These two amplitudes have a statistical correlation of -0.54 in this group whereas for $\mathbf{Q}>7$ Å^{-1} the correlation is -0.06. It would therefore appear that the reflections with $\mathbf{Q}>7$ Å^{-1} are necessary only to discern these two parameters, and that the difference is not one of anharmonicity.

The form of Eq. (8) is appropriate for vibrational behavior of the deuterium atoms. The change for tunneling can be made by replacing $\mathbf{Q}\cdot\boldsymbol{\Delta}_j$ by $\sin(\mathbf{Q}\cdot\boldsymbol{\Delta}_j)$ for the deuterium atoms. A calculation with this modification did not alter any of the mode amplitudes, but lowered B_{11} to 2.7 Å^2. It is apparent that much larger values of $\mathbf{Q}$ are needed to distinguish whether the deuterium atoms are tunneling or vibrating.

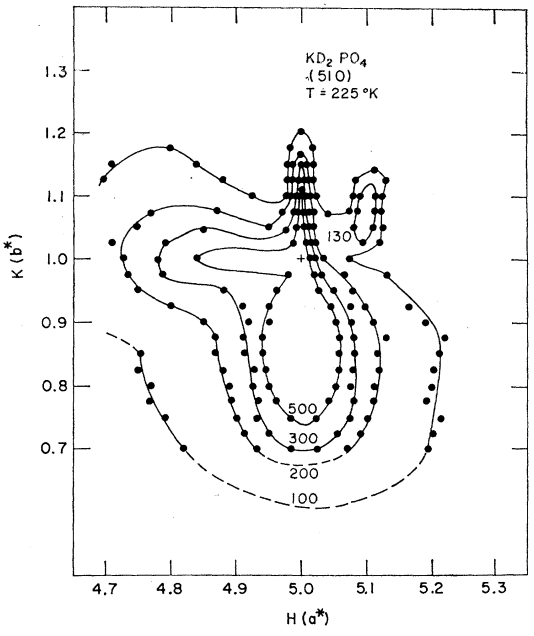

FIG. 10. Intensity contour in the [001] zone near (510) observed with $E=0$.

In the least-squares analysis the positional parameters ($\mathbf{r}_j$) were assumed to be exactly known. The amplitude most sensitive to this assumption is O_c. The position of one oxygen atom has been taken as (0.0829, 0.1490, 0.1270) with the other positions related by symmetry. It is noted that this mode is not determined[36] in the present [010] zone measurements if $z=0.1250$ (a value which would be accidental as it is in no way required by symmetry). The mode determination was therefore evaluated for various values of the oxygen z position. The amplitude is found to be an odd function of ($z=0.1250$) and decreases to 0.013 ± 0.003 and 0.008 ± 0.002 for z values of 0.1290 and 0.1310, respectively. It was observed that the least-squares solution has a high correlation between O_c and the z value of the oxygen, and the resulting values of the weighted variance change by less than 1%. If, however, the accidental value $z=0.1250$ is used in the analysis, the resulting

TABLE II. Ferroelectric mode parameters.

B_{11}	3.4±0.2 Å^2
$B_{22}=B_{33}$	2.3±0.3 Å^2
K_z	0.0066±0.0005c
P_z	−0.0055±0.0006c
O_z	−0.0008±0.0005c
D_z	−0.011±0.001c
D_a	0.025±0.001a
O_b	0.0002±0.0002a
O_c	0.026±0.007a

[35] V. Ambegaokar, J. M. Conway, and G. Baym, in *Lattice Dynamics*, edited by R. F. Wallis (Pergamon Press, Inc., New York, 1965), p. 261.

[36] This point was first brought to our attention by W. Cochran.

value of the weighted variance is 2.6 with O_c being indeterminate. This compares with the value 2.1 which obtains when $z \neq 0.1250$ and a value is determined for O_c.

VI. CONCLUDING REMARKS

The model described by Table II is quite like the Cochran mode depicted in Fig. 2. That such motions are concerned with the ferroelectric soft mode are here proven conclusively. A striking result not heretofore considered in discussions of the ferroelectric mode is the large distortional movement of the oxygen tetrahedra due to O_c. Additionally, a rather large motion of the deuterium atoms takes place along the c axis. A particular force model predicting the motion of the ferroelectric mode has not been obtained.

Although the principal features of the Cochran model for KH_2PO_4 are confirmed here for KD_2PO_4, it is evident that the soft ferroelectric mode in KD_2PO_4 cannot be predicted quantitatively and in detail from structural changes that occur at the transition in KH_2PO_4. The data of Bacon and Pease[11] admit no x-y distortion of the oxygen tetrahedra due to the transition. Additionally, it is noted that the structural change in KH_2PO_4 indicates a movement of the hydrogen atoms along the c axis in phase with the K atoms. The present work indicates the deuterium atoms move along the c axis in phase with the P atoms. One possible explanation is that, in these respects, the soft mode found here for KD_2PO_4 is intrinsically different in its atomic movements from the soft mode in KH_2PO_4. If the soft mode in KD_2PO_4 condenses, the positional parameters of the atoms in the low-temperature phase of KD_2PO_4 may therefore differ from those of KH_2PO_4.

One may speculate, however, that the soft modes are similar and do condense into the low-temperature structure immediately below the transformation temperature, but as the temperature is dropped the distortion due to O_c relaxes. This could take place without another transition occurring as the O_c movement now belongs to the Γ_1 representation of the low-temperature phase. The x-ray measurements on KH_2PO_4 of Frazer and Pepinsky[10] would appear not to support this possibility, as their analysis indicated no x-y movement of the oxygen tetrahedra as close as 6°K below T_c.

The scattering intensity of the overdamped soft phonon as measured in the [010] zone and depicted in Figs. 7 and 9 appears to be of the form attributable to critical scattering. In light of measurements in the [001] zone as depicted in Fig. 10, $F_i(\mathbf{Q})$ changes in such rapid fashion as to preclude an analysis of the data in terms of a correlation length. A physical insight into the apparent slow variation of $F_i(\mathbf{Q})$ in the [010] zone compared with the [001] zone does not present itself. A similar slow variation of $F_i(\mathbf{Q})$ for the antiferroelectric soft mode in $ND_4D_2PO_4$ was observed in a neutron investigation of the [010] zone by Meister *et al.*[37]

It is noted in the data of Table I that the odd-l reflections are generally more intense than for l even. One can expect that a periodicity in l occurs as there exists very nearly a finite structure zone in the c direction of four Brillouin zones in breadth. Additionally, the opposing motions in the z direction of the K and P atoms result in contributions to $F_i(\mathbf{Q})$ that cancel for l even and are reinforced for odd l.

The elastic compliance $(C_{66}{}^E)^{-1}$ has been measured for KD_2PO_4 by Sliker and Burlage[30] at room temperature. If the thermal behavior and difference between $C_{66}{}^E$ and $C_{66}{}^D$ in KD_2PO_4 is similar to that of KH_2PO_4, their value of 6.06×10^{10} dyn/cm^2 is lower than that obtained by neutron measurement. It is possible that the neutron measurement is not quantitatively similar to $C_{66}{}^D$ due to the high frequency at which the measurement takes place.

ACKNOWLEDGMENTS

The authors would like to acknowledge J. D. Axe, M. Blume, Y. Yamada, and W. Cochran for many stimulating discussions.

[37] H. Meister, J. Skalyo, Jr., B. C. Frazer, and G. Shirane, Phys. Rev. **184**, 550 (1969).